Available online at www.sciencedirect.com
ScienceDirect
Ceramics International 36 (2010) 173–179
CERAMICS INTERNATIONAL
www.elsevier.com/locate/ceramint

Crack profiles under a Vickers indent in silicon nitride ceramics with various microstructures

Hiroyuki Miyazaki *, Hideki Hyuga, Yu-ichi Yoshizawa, Kiyoshi Hirao, Tatsuki Ohji

National Institute of Advanced Industrial Science and Technology (AIST), Anagahora 2266-98, Shimo-shidami, Moriyama-ku, Nagoya 463-8560, Japan

Received 25 May 2009; received in revised form 3 June 2009; accepted 7 July 2009
Available online 11 August 2009

Abstract

The effect of microstructure on crack morphology under a Vickers indentation was studied using 20 various silicon nitride ceramics including bearing-grade silicon nitrides. The indentation load was decreased from 98 N to 9.8 N and a transition of the crack types from half-penny crack to radial one was observed with both decoration method and serial sectioning technique. All of the indented samples possessed the half-penny cracks at the load of 98 N. The transition of crack profiles in the samples with coarse microstructure occurred when the load decreased from 49 N to 19.6 N, whereas the transition load for the sample with fine microstructure was ~9.8 N. Half-penny cracks were formed regardless of the microstructures when the ratio of the half of crack length to the half of diagonal size of an indentation, *c*/*a*, was above ~2. The dependence of the transition load on both Vickers hardness and fracture resistances was analyzed using Pajares's equation.

Keywords: C. Toughness and toughening; C. Hardness; D. Si_3N_4; Indentation fracture technique

1. Introduction

Silicon nitride ceramics have excellent tolerance during the usage in sever conditions, which makes them applicable to tribological parts such as bearings for hard disks and mechanical seals [1]. For such applications, it is necessary to evaluate their fracture toughness from real parts themselves. However, conventional toughness evaluation methods such as single-edge-precracked beam (SEPB) [2,3] and surface flaw in flexure (SCF) methods [4] are difficult to apply since the sizes of tribological parts such as bearings are mostly smaller than the test specimens specified in these methods. Thus, the indentation fracture (IF) method, which has been proposed by Lawn et al. [5], is one of the most effective solutions for the need of measuring the fracture resistance of the small ceramic materials.

It is widely known that the type of cracks transits from radial cracks (also referred as Palmqvist-cracks) to half-penny (or median) cracks as the indentation load increases [6–9]. These crack systems must be distinguished before the application of the IF technique. Niihara et al. estimated that this transition occurred when the ratio of the length of surface crack, 2*c* to diagonal size of the indent, 2*a* becomes larger than 2.5 [6]. They proposed that the type of cracks should be identified from the numerical *c*/*a* values. However, investigations of the crack morphology of ceramics by decoration technique and/or by layer-by-layer removal method showed different critical *c*/*a* values for different ceramics [7–9]. Jones et al. demonstrated the critical *c*/*a* ratio for alumina was about 2 and differed from that for 3Y-TZP, *c*/*a* = ~3 [7]. In the case of 4Y-PSZ, Pajares et al. reported that the critical value of *c*/*a* was 3.4 [8]. Observation of indentation crack profiles in silicon nitride by Lube suggested that the critical value of *c*/*a* was between 1.8 and 2.2 [9]. Therefore, crack-profile shapes of various kinds of ceramics cannot be inferred from the constant *c*/*a* value as pointed out by Jones et al. [7].

Mechanical properties such as strength and fracture resistance of silicon nitrides have been improved greatly through microstructural designs so called ''self-reinforcement'' mechanisms [10–15]. It is likely that the *c*/*a* value for the transition of crack type also differs from one sample to another if the microstructures are considerably different. However, the

* Corresponding author. Tel.: +81 52 736 7486; fax: +81 52 736 7405.
E-mail address: h-miyazaki@aist.go.jp (H. Miyazaki).

0272-8842/$36.00
doi:10.1016/j.ceramint.2009.07.016

effect of microstructure on the shape of cracks in a certain ceramics has been scarcely studied. Thus, the first aim of this study is to clarify the dependence of the critical *c*/*a* value on the microstructure of various types of silicon nitride ceramics.

The critical indentation load for the transition of crack system is also of great importance, since the test load must be specified in the standards such as ASTM F2094 which adopts IF method [16]. Pajares et al. reported that the transition load for yttria stabilized zirconia varied significantly depending on both fracture toughness and hardness [8]. They correlated the transition load, P^* with toughness, K_R and hardness H as follows:

$$P* = \left(\frac{8m^6}{\chi^4}\right)\left(\frac{K_R^4}{H^3}\right) \quad (1)$$

where m and χ are material constants. The equation was proposed in their model which combined the observed geometrical features of cracks in 4Y-PSZ with residual stress consideration. The constant m is a minimum value of the ratio of $c/2a$ where a transition from radial to the half-penny cracks occurs. χ is often expressed by the relation $\chi = \xi f(E/H)$ with ξ being a dimensionless constant, and E and H being Young's modulus and hardness, respectively. The equation shows that the transition load, P^* is proportional to K_R^4/H^3, which means that the crack system at a constant test load may vary when toughness and hardness of ceramics differ from one sample to another. In such cases, it is necessary to assure that the test load specified in the standard is above the critical load P^* to form half-penny system regardless of the microstructure and/or toughness and hardness of silicon nitrides. Accordingly, the second subject of this report is to study the effect of microstructure on the transition load.

In this study, the crack systems of three representative silicon nitrides were fully investigated by both decoration and serial sectioning techniques to clarify the relation between the transition of crack type and the microstructures. Then, 17 silicon nitrides with different microstructures including ball-bearing-grade silicon nitrides were employed to check the critical values of both *c*/*a* and test load determined by the full observation of the first three samples.

2. Experimental procedure

2.1. Materials

Twelve kinds of silicon nitrides were hot-pressed using Si_3N_4 powder with Y_2O_3 and Al_2O_3 as sintering additives, which were categorized into three groups. The amounts of the sintering additives of the first two sets of samples were fixed at 2.5 wt% Al_2O_3 and 2.5 wt% Y_2O_3 (A group) and 5 wt% Al_2O_3 and 5 wt% Y_2O_3 (B group) as listed in Table 1. The sintering temperature and soaking time of these samples were varied as follows: 1750 °C for 1 h, 1850 °C for 1 h, 1950 °C for 2 h and 1950 °C for 8 h. By contrast, the amount of the additives of the last set of samples was changed from 1 wt% Al_2O_3 and 1 wt% Y_2O_3 to 10 wt% Al_2O_3 and 10 wt% Y_2O_3 while the sintering condition was set constant at 1950 °C for 2 h. The detailed fabrication procedure was described in our previous papers [17,18]. Silicon nitrides from commercial sources were also used as test materials. Material identifications and their suppliers are listed in Table 2. In this study, the materials for bearing-grade are referenced by the code such as BG1–BG4 to retain anonymity. The materials for other purposes are also denoted by OP1–OP4 for the same reason.

Considerable variation in the microstructures was observed for these samples. The representative microstructures observed by scanning electron microscopy (SEM) are shown in Fig. 1. The C1 sample which was sintered with the least additives at 1950 °C for 2 h consisted of fine and uniform grains, whereas extraordinary large elongated grains (>6 μm) existed occasionally in the sample sintered at 1950 °C for 8 h (B4). In the case of bearing-grade silicon nitrides (BG2), rod-like grains were distributed among fine equiaxed grains. Other bearing-grade samples also showed a similar microstructure. By contrast, the microstructures of the silicon nitrides for other

Table 1
Composition, sintering condition and mechanical properties of the silicon nitride samples fabricated by the authors.

Material code	Additives (wt%)		Sintering temperature (°C)	Soak time (h)	Young's modulus[a] (GPa)	Vicker's hardness[b] (GPa)	Fracture resistance[b,c] (MPa $m^{1/2}$)
	Al_2O_3	Y_2O_3					
A1	2.5	2.5	1750	1	309	16.3	4.6
A2	2.5	2.5	1850	1	309	16.0	4.8
A3	2.5	2.5	1950	2	309	14.9	5.5
A4	2.5	2.5	1950	8	310	14.3	5.4
B1	5.0	5.0	1750	1	299	15.4	5.0
B2	5.0	5.0	1850	1	299	15.0	5.1
B3	5.0	5.0	1950	2	300	14.3	5.8
B4	5.0	5.0	1950	8	306	13.7	5.9
C1	1.0	1.0	1950	2	315	16.4	4.0
C2	1.75	1.75	1950	2	312	15.8	4.5
C3	3.34	3.34	1950	2	307	14.9	5.7
C4	10.0	10.0	1950	2	280	13.7	5.5

[a] Young's modulus was measured by the ultrasonic pulse echo method.
[b] Vicker's hardness and fracture resistance were obtained at an indentation load of 98 N.
[c] Fracture resistance was calculated according to the Japanese Industrial Standard, JIS R 1607.

Table 2
Alphabetical listing of commercially available silicon nitrides used in this study.

Material identification	Supplier name
EC141	NGK Spark Plug
NBD200	Saint Gobain
SN1	Japan Fine Ceramic Center
SN101C	Saint Gobain
SN220	Kyocera
SN240	Kyocera
SUN12	Nikkato
TSN03NH	Toshiba Materials

purpose were dissimilar to each other. For example, the microstructure of the OP3 sample was characterized by needle-like grains, whereas the others were not.

These microstructural features were reflected to the mechanical properties, such as elastic modulus, Vickers hardness and fracture resistance as shown in Tables 1 and 3. The fracture toughness of samples in both A and B groups increased with sintering temperature and/or soaking time (Table 1), which is attributable to the development of rod-like grains as mentioned above. Both elastic modulus and hardness decreased with an increment in the additive contents for the C group. Young's modulus and hardness of the bearing-grade samples were apparently higher than those of the rest commercial samples (Table 3). The fracture resistance of the former samples showed relatively higher value than those of the latter samples except the OP3 sample, as well. Quantitative analysis of microstructures for some selected samples together with its relation to the mechanical properties can be found in our previous studies [17–19].

Table 3
Mechanical properties of the commercially available silicon nitride samples.

Material code	Young's modulus[a] (GPa)	Vicker's hardness[b] (GPa)	Fracture resistance[b,c] (MPa $m^{1/2}$)
BG1	305	15.1	4.9
BG2	310	14.6	4.8
BG3	309	15.7	5.6
BG4	314	15.2	4.8
OP1	289	12.6	4.4
OP2	286	13.3	4.4
OP3	284	13.5	5.1
OP4	295	13.6	4.7

[a] Young's modulus was measured by the ultrasonic pulse echo method.
[b] Vicker's hardness and fracture resistance were obtained at an indentation load of 98 N.
[c] Fracture resistance was calculated according to the Japanese Industrial Standard, JIS R 1607.

2.2. Test procedure

Vickers indentations were made on polished surfaces with a hardness tester (Model AVK-C2, Akashi Corp., Yokohama, Japan). In the case of self-made samples, the polished surface perpendicular to the hot-pressing axis was used for indentations. The indentation contact time was 15 s. Indentation loads of 9.8 N, 19.6 N, 49 N and 98 N were chosen to vary the crack type. Bright field images were observed with a 10× eyepiece and a 50× objective using a travelling microscope (Model MM-40, Nikon Corp., Tokyo, Japan). The lengths of the impression diagonals, 2*a*, and surface cracks, 2*c*, were measured immediately after the indentation. Only indentations whose four primary

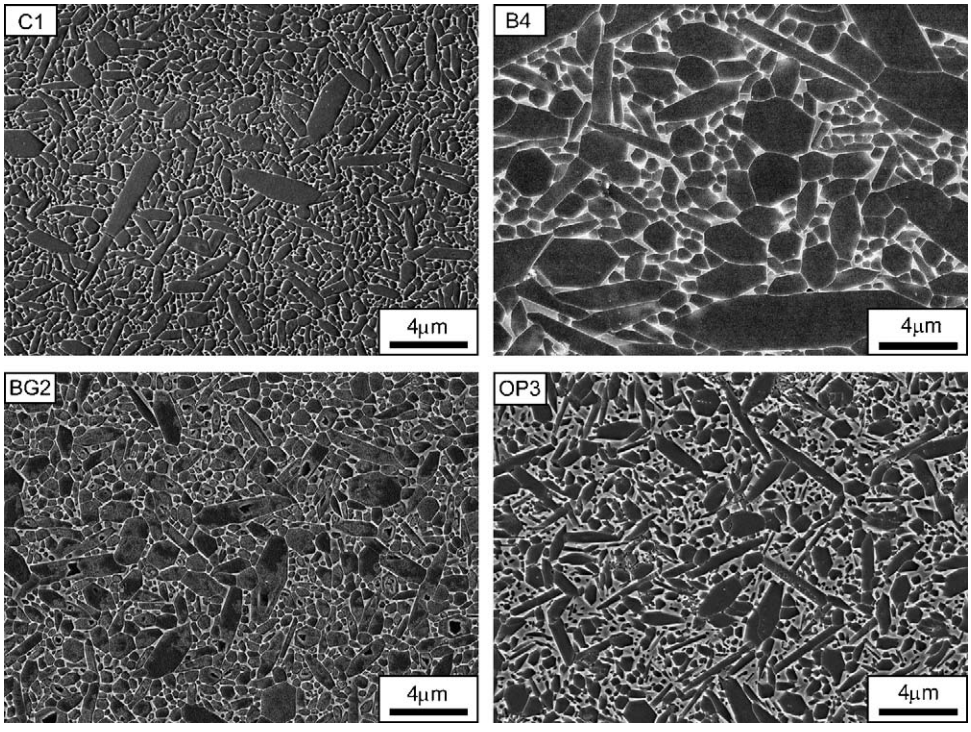

Fig. 1. Example of SEM micrographs of the polished and etched surfaces of silicon nitride ceramics.

cracks emanated straight forward from each corner were accepted. Indentations with badly split cracks or with gross chipping were rejected. Eight impressions were made at each load. Nearly all the indentations were acceptable. The counter of the indentation cracks was assessed by stepwise polishing and measuring the surface length of the cracks as a function of depth.

Decorating indentation cracks with red dye was also applied to observe the crack geometries. The method was originally proposed by Jones et al. [7], but in this study, red dye and optical microscopy were used instead of lead acetate solution and SEM. The indentations were made on the center of the mirror finished tensile surface of flexural specimens. After the indentation, a drop of red dye was placed on the indentation immediately, followed by drying for 10–20 min. The specimens were broken in flexure mode with the original indentation crack acting as failure origin. The fracture surface was observed with the optical microscope. Environmental slow crack growth during the test was not expected since the red dye was non-water-based solution and Si_3N_4 is unsusceptible to the slow crack growth [20,21]. The possible disadvantage of the method

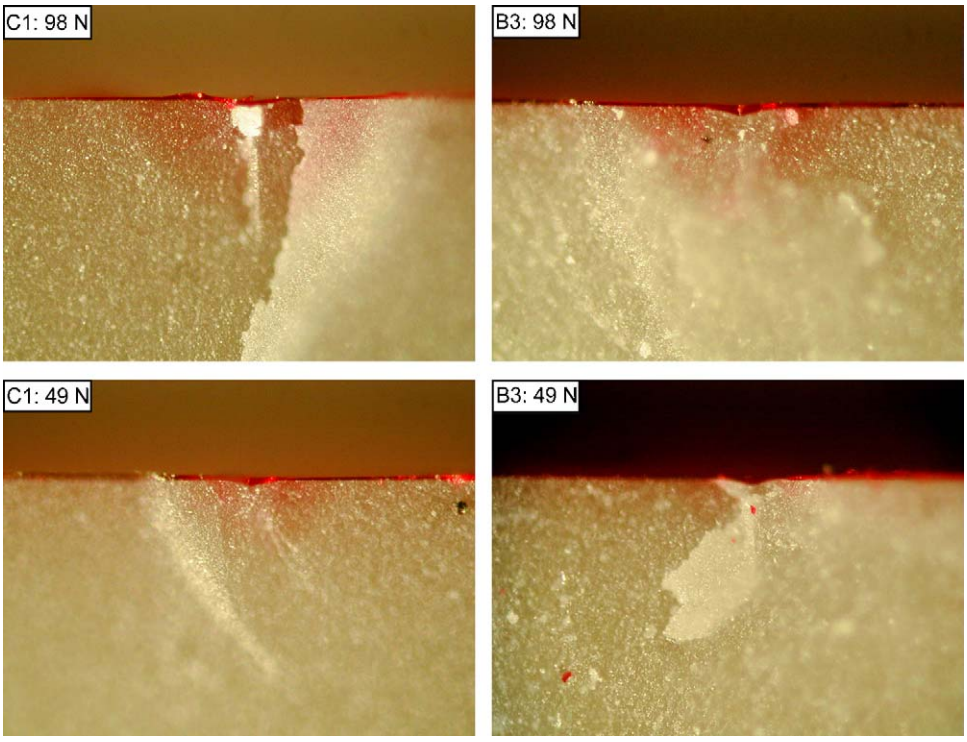

Fig. 2. Crack profiles of indentations in the C1 and B3 samples at 98 N and 49 N observed by the decoration method using optical microscopy.

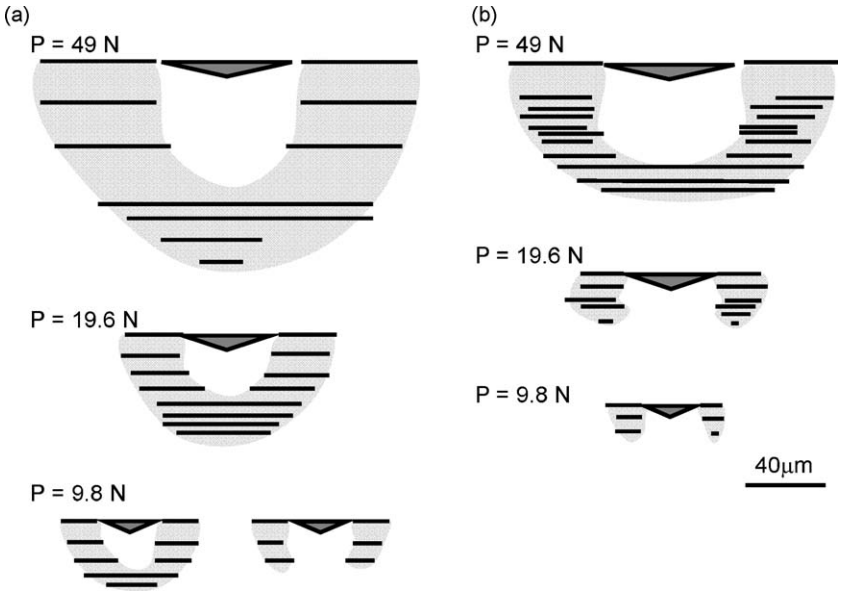

Fig. 3. Indentation crack profile as determined by serial sectioning of Vickers indents at the load of 49 N and less: (a) for the C1 sample and (b) for the B3 sample.

Table 4
Variation of crack shape parameters with load for three representative silicon nitride ceramics.

Material code	Load (N)	c (μm)	a (μm)	c/a	Crack profile
B3	98	125.1	56.4	2.22 (0.04)	Half-penny
	49	83.8	40.1	2.09 (0.05)	Half-penny
	19.6	47.1	25.5	1.86 (0.05)	Radial
	9.8	29.0	17.3	1.67 (0.04)	Radial
B4	98	127.1	57.6	2.20 (0.05)	Half-penny
	49	84.4	40.9	2.09 (0.03)	Half-penny
	19.6	47.5	25.8	1.85 (0.08)	Radial
	9.8	27.5	17.7	1.55 (0.02)	Radial
C1	98	155.2	52.6	2.95 (0.06)	Half-penny
	49	99.8	37.9	2.65 (0.06)	Half-penny
	19.6	53.8	24.0	2.24 (0.07)	Half-penny
	9.8	33.8	15.8	2.14 (0.03)	Half-penny and Radial

is that the crack extension may be slightly underestimated due to the insufficient infiltration of the dye into the crack tips.

3. Results and discussion

3.1. Full observation of the crack system in three representative silicon nitrides with different microstructures

Three representative silicon nitrides with different microstructures, C1, B3 and B4, each of which possessed the fine microstructure, medium one and the coarsest one respectively, were selected to investigate the effects of microstructure on both transition load and the critical c/a values. The crack-profile shapes observed by the optical microscope are shown in Fig. 2 for the C1 and B3 samples indented at the load of 98 N and 49 N. The profiles of both cracks at 98 N were half-penny types. The crack of the C1 sample at 49 N was recognized as half-penny type, while that of the B3 sample was unclear. The crack profiles for the B4 samples at both loads were similar to those of the B3 sample.

Fig. 3 shows the results of serial sectioning for the C1 and B3 samples at the load of 49 N and less. Half-penny cracks were formed in the C1 sample at the loads of 49 N and 19.6 N. When the sample was indented at 9.8 N, both half-penny and radial-type cracks coexisted, 2/3 of the cracks were half-penny type and the rest were radial ones. Thus, the transition load for the C1 sample was ∼9.8 N. By contrast, serial sectioning of the indentations in the B3 samples revealed that the crack pattern transited from half-penny to radial ones when the load decreased from 49 N to 19.6 N. The transition for the B4 sample also occurred at the same range of loads.

The c/a values for the indentation in the three samples at each load are presented in Table 4 together with the crack types. Each c/a value is the mean of ∼8 indentations. The standard deviation for each c/a value is shown in parentheses. It was found that the critical c/a value was almost independent on the microstructures of silicon nitrides and was between 1.8 and 2.2, whereas the transition loads for coarse samples (B3 and B4) were at least two times larger than that for the sample with fine microstructure (C1).

3.2. Observation of crack system in other silicon nitrides with various microstructures

In order to confirm the critical c/a value and the dependence of transition load on the microstructures, many kinds of silicon nitrides were employed as test materials. Examples of the

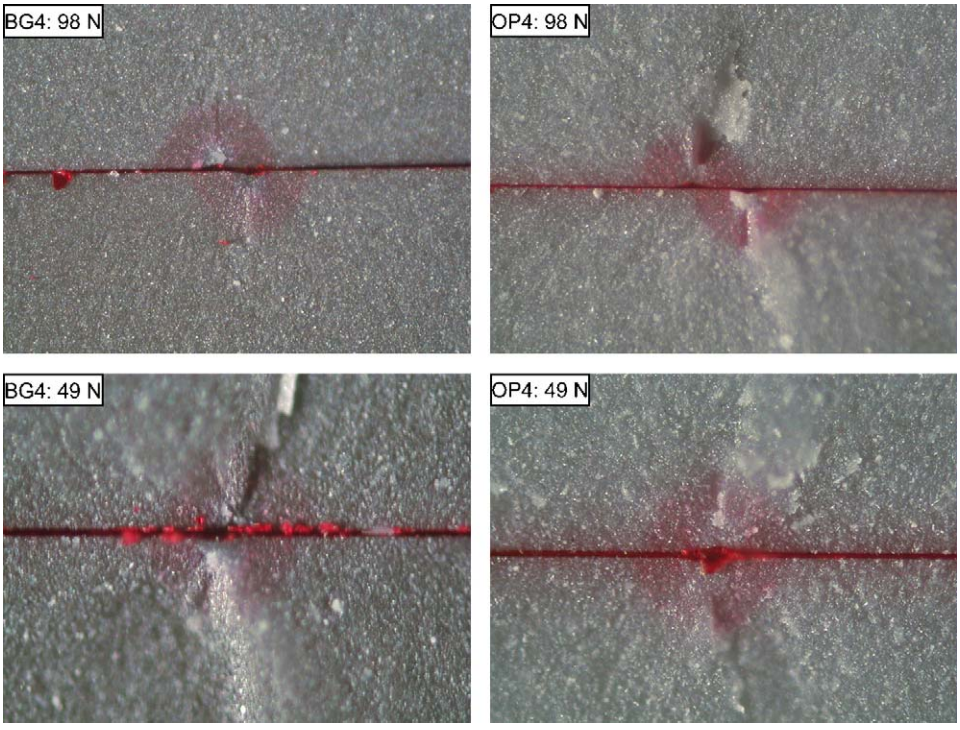

Fig. 4. Optical photos of both halves in the BG4 and OP4 samples indented at 98 N and 49 N and observed by the decoration method.

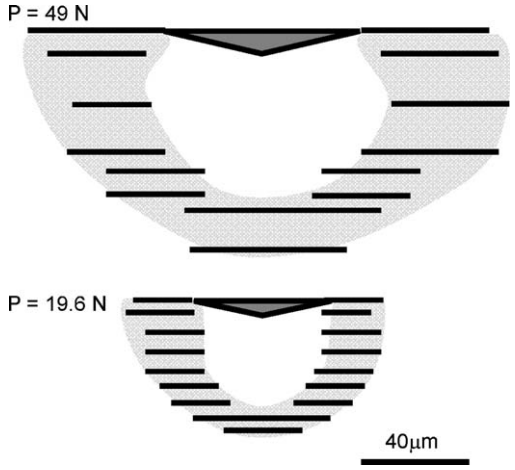

Fig. 5. Indentation crack profile as determined by serial sectioning of Vickers indents in the BG2 sample at the load of 49 N and 19.6 N.

optical images for the cracks observed at the fracture surfaces are shown in Fig. 4. The profiles of cracks in both BG4 and OP4 samples at the loads of 98 N and 49 N were half-penny type. The crack profiles for other samples at 98 N were also identified as half-penny type. The A1, A2, B1, B2, C2, BG3 and OP3 samples exhibited half-penny cracks when the indentation load was 49 N, while the rest samples had ambiguous crack morphology similar to the crack in the B3 sample indented at 49 N (Fig. 2). The serial sectioning method was applied further for both BG1 sample indented at 49 N and BG2 samples indented at 49 N and 19.6 N. The indentations at 49 N in the BG1 sample exhibited half-penny cracks. In the case the BG2 sample, all of the cracks at 49 N and 19.6 N were identified as the half-penny type as illustrated in Fig. 5.

Ratios of half crack length to half of diagonal size are listed in Tables 5 and 6 for self-made samples and those from commercial source, respectively. The standard deviations were in the range of

Table 5
Ratios of half crack length, c to half of diagonal size, a for half-penny cracks in the self-made samples at each indentation load.

Load (N)	Material code								
	A1	A2	A3	A4	B1	B2	C2	C3	C4
98	2.69	2.58	2.34	2.34	2.58	2.43	2.69	2.27	2.24
49	2.40	2.32	2.15[a]	2.08[a]	2.31	2.18	2.45	2.09[a]	2.04[a]

[a] Un-identified cracks.

Table 6
Ratios of half crack length, c to half of diagonal size, a for half-penny cracks in the samples from commercial source at each indentation load.

Load (N)	Material code							
	BG1	BG2	BG3	BG4	OP1	OP2	OP3	OP4
98	2.52	2.54	2.34	2.59	2.57	2.42	2.22	2.51
49	2.38 [b]	2.36[b]	2.20	2.40	2.37[a]	2.09[a]	2.11	2.39
19.6	–	2.23[b]	–	–	–	–	–	–

[a] Un-identified cracks.
[b] The crack profile was observed using serial sectioning technique, while others were identified using decoration method.

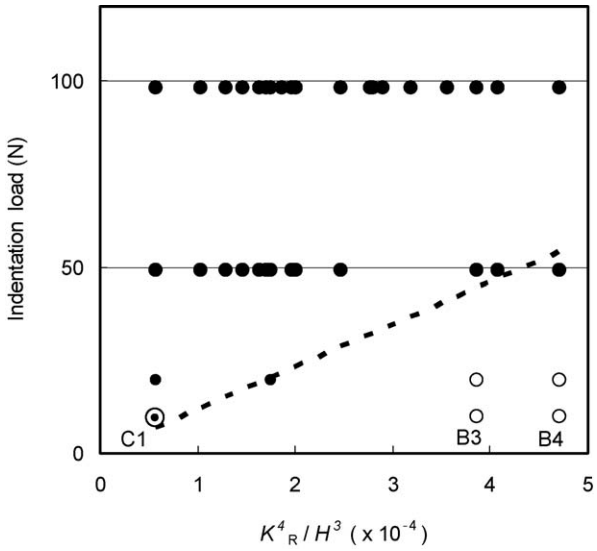

Fig. 6. Crack types plotted on the map of indentation load versus K_R^4/H^3. Closed circles represent half-penny cracks, while open circles denote radial ones. Co-existence of both types is indicated by the circle with dot. The dotted line represents the estimated transition load from half-penny to radial cracks, which was calculated by Eq. (1) using the data of the B4 sample.

0.02–0.09. All these c/a values for the half-penny cracks were larger than 2, which confirmed that the critical c/a value for the transition lies in ∼2 regardless of the microstructures.

The types of identified cracks for all of the silicon nitride samples were plotted on the map of indentation load versus K_R^4/H^3 in Fig. 6. When K_R^4/H^3 was small, half-penny cracks were dominant and radial cracks appeared only at the load of 9.8 N (C1 sample). By contrast, radial cracks were identified at the load of 19.6 N when K_R^4/H^3 was larger (B3 and B4 samples), implying the transition load from radial to half-penny types increased with K_R^4/H^3. The line in the figure represents the transition load calculated using Eq. (1) with the data of the B4 sample. It appeared that all of the data points for half-penny cracks resided above or on the line, which verified the rough estimation of transition load using Eq. (1). It should be noted that the estimated transition load barely exceeded 49 N, indicating that indentation at 49 N or more surely generates half-penny cracks.

4. Conclusion

We would conclude that: (1) crack-profile shape of silicon nitride can be inferred from c/a ratios because of the independence of critical c/a value on the microstructure, (2) when the load is 49 N and more, the half-penny crack is dominant, and (3) the estimation of transition load with Pajares's equation is valid for various kinds of silicon nitride. Consequently, the indentation load of 196 N, which is specified in ASTM F2094, is sufficient level for correct measurements of indentation fracture resistance of silicon nitride ceramics.

Acknowledgements

This work has been supported by METI, Japan, as part of the International Standardization Project of Test Methods for

rolling contact fatigue and fracture resistance of ceramics for ball bearings.

References

[1] K. Komeya, Material development and wear applications of Si_3N_4 ceramics, Ceram. Trans. 133 (2002) 3–16.

[2] T. Nose, T. Fujii, Evaluation of fracture toughness for ceramic materials by a single-edge-precracked-beam method, J. Am. Ceram. Soc. 71 (1988) 328–333.

[3] Testing methods for fracture toughness of fine ceramics, Japanese Industrial Standard, JIS R 1607 1995.

[4] Fine ceramics (advanced ceramics, advanced technical ceramics)—determination of fracture toughness of monolithic ceramics at room temperature by the surface crack in flexure (SCF) method, International Organization for Standards, ISO 18756 2003 Geneva.

[5] B.R. Lawn, A.G. Evans, B. Marshall, Elastic/plastic indentation damage in ceramics: the median/radial crack system, J. Am. Ceram. Soc. 63 (1980) 574–581.

[6] K. Niihara, R. Morena, D.P.H. Hasselman, Evaluation of K_{Ic} of brittle solids by the indentation method with low crack-to-indent ratios, J. Mater. Sci. Lett. 1 (1982) 13–16.

[7] S.L. Jones, C.J. Norman, R. Shahani, Crack-profile shapes formed under a Vickers indent pyramid, J. Mater. Sci. Lett. 6 (1987) 721–723.

[8] A. Pajares, F. Guiberteau, F.L. Cumbrera, R.W. Steinbrech, A. Dominguez-Rodriguez, Analysis of kidney-shaped indentation cracks in 4Y-PSZ, Acta Mater. 44 (11) (1996) 4387–4394.

[9] T. Lube, Indentation crack profiles in silicon nitride, J. Eur. Ceram. Soc. 21 (2001) 211–218.

[10] E. Tani, S. Umebayashi, K. Kishi, K. Kobayashi, M. Nishijima, Gas-pressure sintering of Si_3N_4 with concurrent addition of Al_2O_3 and 5 wt% rare earth oxide: high fracture toughness Si_3N_4 with fiber-like structure, Am. Ceram. Soc. Bull. 65 (1986) 1311–1315.

[11] T. Kawashima, H. Okamoto, H. Yamamoto, A. Kitamura, Grain size dependence of the fracture toughness of silicon nitride ceramics, J. Ceram. Soc. Jpn. 99 (1991) 320–323.

[12] N. Hirosaki, Y. Akimune, M. Mitomo, Effect of grain growth of β-silicon nitride on strength, Weibull modulus, and fracture toughness, J. Am. Ceram. Soc. 76 (1993) 1892–1894.

[13] P.F. Becher, Microstructural design of toughened ceramics, J. Am. Ceram. Soc. 74 (1991) 255–269.

[14] R.W. Steinbrech, Toughening mechanisms for ceramic materials, J. Eur. Ceram. Soc. 10 (1992) 131–142.

[15] T. Ohji, K. Hirao, S. Kanzaki, Fracture resistance behavior of highly anisotoropic silicon nitride, J. Am. Ceram. Soc. 78 (1995) 3125–3128.

[16] Standard Specification for Silicon Nitride Bearing Balls, ASTM F 2094-03a, 2003.

[17] H. Hyuga, S. Sakaguchi, K. Hirao, Y. Yamauchi, S. Kanzaki, Influence of microstructure and grain boundary phase on tribological properties of Si_3N_4 ceramics, Ceram. Eng. Sci. Proc. 22 (2001) 197–202.

[18] H. Miyazaki, H. Hyuga, K. Hirao, T. Ohji, Comparison of fracture resistance as measured by the indentation fracture method and fracture toughness determined by the single-edge-precracked beam technique using silicon nitrides with different microstructures, J. Eur. Ceram. Soc. 27 (2007) 2347–2354.

[19] H. Miyazaki, H. Hyuga, Y. Yoshizawa, K. Hirao, T. Ohji, Relationship between fracture toughness determined by surface crack in flexure and fracture resistance measured by indentation fracture for silicon nitride ceramics with various microstructures, Ceram. Int. 35 (2009) 493–501.

[20] K.D. McHenry, T. Yonushonis, R.E. Tressler, Low-temperature subcritical crack growth in SiC and Si_3N_4, J. Am. Ceram. Soc. 59 (1976) 262–263.

[21] A. Bhatnagar, M.J. Hoffman, R.H. Dauskardt, Fracture and subcritical crack-growth behavior of Y–Si–Al–O–N glasses and Si_3N_4 ceramics, J. Am. Ceram. Soc. 83 (2000) 585–596.